INTERNATIONAL JOURNAL FOR NUMERICAL AND ANALYTICAL METHODS IN GEOMECHANICS
Int. J. Numer. Anal. Meth. Geomech., 2000; **24**:991–1011

A semi-empirical method for the liquefaction analysis of offshore foundations

H. A. Taiebat*,† and J. P. Carter‡

Department of Civil Engineering, The University of Sydney, NSW 2006, Australia

SUMMARY

This paper presents a relatively simple method for three-dimensional liquefaction analysis of granular soil under offshore foundations. In this method, the Mohr–Coulomb model, which defines the elasto–plastic stress–strain relationship under monotonic loading, is modified to accommodate the plastic strains generated by cyclic loading. The effects of cyclic loading, evaluated from the results of laboratory tests on saturated samples of soil, are incorporated into the model. The method is implemented in an efficient finite element program for analyses of three-dimensional consolidating soil. The practicability of the model is demonstrated by analysis of a typical offshore foundation, and the predictions of the numerical analysis are compared with the observed behaviour of the foundation. Copyright © 2000 John Wiley & Sons, Ltd.

KEY WORDS: liquefaction analysis; offshore foundations; 3-D finite element

1. INTRODUCTION

Foundations for marine structures are generally subjected to cyclic loads due to wave forces applied during a storm. These loads usually include a large number of cycles of short-to-medium periods (5–15 s) with variable amplitude. Laboratory tests on samples of granular soils show that application of a large number of cyclic loads with moderate amplitude can produce a progressive degradation of the soil resistance, which can alter the stability of marine structures founded on them. It is therefore essential to consider these kinds of loads in the design of marine foundations.

Liquefaction analysis of offshore foundations under cyclic loads can be performed by at least two numerical approaches. The first approach is to use a complex constitutive model capable of predicting the additional effects of cyclic loading. Phenomena such as permanent volumetric strains (densification) or generation of pore pressures, which occur after each cycle of load, should

*Correspondence to: H. A. Taiebat, Research Student The University of Sydney, Australia
†Research Student
‡Challis Professor of Civil Engineering

Contract/grant sponsor: Centre for Geotechnical Research
Contract/grant sponsor: Australian Research Council

Received 16 August 1999
Revised 7 April 2000

be included in the constitutive equations. Many sophisticated models have been developed for this purpose but they mostly require the specification of numerous model parameters, many of which are usually difficult to determine. Furthermore, an incremental method is usually required for repeated solution of the non-linear governing equations offered by these models, using a large number of calculation steps to analyse each cycle of loading. Application of these models for liquefaction analysis of an offshore foundation, typically involving hundreds if not thousands of load cycles, usually requires excessive computational effort.

In the second approach, a simpler methodology is adopted, and this usually implies further approximation of the real soil behaviour. Conventional constitutive models, suitable for monotonic loading, are retained and the effects of cyclic loading are incorporated independently. This method is based on an experimental determination of soil behaviour under a large number of cycles, including measurements of the evolution of strain and pore pressure generation with cyclic loading. Such an approach has the advantage of simplicity and the most direct use of the experimental data. This simpler approach has been adopted in this study to develop a practical method for liquefaction analysis of foundations under cyclic loading.

2. EFFECTS OF CYCLIC LOADING ON GRANULAR SOILS

The most common effect of cyclic loading on granular soil is the tendency for cumulative densification and reduction of void space in the soil. For undrained conditions this tendency increases the pore water pressure, and when drainage is permitted volumetric strains and the associated displacements increase.

In the most commonly conducted cyclic undrained triaxial tests on saturated samples of granular soils, the average values of the mean total stress and the deviatoric stress are usually maintained constant. During cyclic loading, excess pore pressures are generated causing a corresponding change in the average value of the mean effective stress. This change is represented in the Cambridge p'–q space in Figure 1, where p' is the mean effective stress and q is the deviatoric shear stress. The stress components p' and q are defined as follows in terms of the principal effective stress components $(\sigma'_1, \sigma'_2, \sigma'_3)$, i.e.

$$p' = \tfrac{1}{3}(\sigma'_1 + \sigma'_2 + \sigma'_3)$$

and

$$q = \frac{1}{\sqrt{2}}\sqrt{(\sigma'_1 - \sigma'_2)^2 + (\sigma'_2 - \sigma'_3)^2 + (\sigma'_3 - \sigma'_1)^2}$$

In Figure 1 u_c is the pore pressure generated by cyclic loading and u_{max} is the maximum achievable pore pressure before failure, i.e. the horizontal distance between the initial state of stress and the failure surface.

During cyclic loading the state of effective stress moves toward the deviatoric axis, reducing the shearing resistance of the soil, and may eventually reach the failure envelope. At this state the shearing resistance of the soil grains is fully mobilized and may even diminish, and this often results in the soil flowing like a viscous liquid. When this condition is reached, liquefaction is said to have occurred.

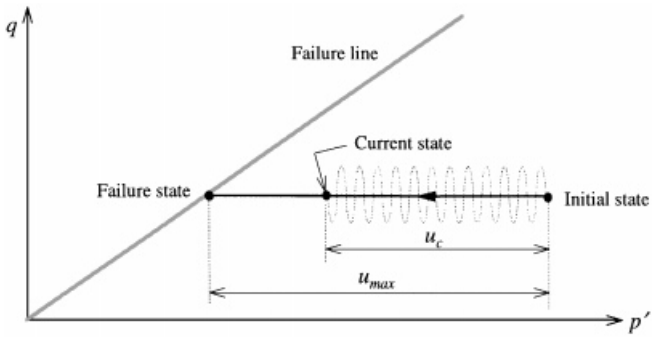

Figure 1. Stress path in an undrained triaxial test on saturated sand.

From the many results of undrained cyclic tests on saturated samples of granular soil that have been reported, two main characteristics are most commonly measured. The first is the relationship between the cyclic stress ratio and the number of cycles required for liquefaction failure. The cyclic stress ratio (q_c/p'_i) defines the relative magnitude of cyclic deviatoric stress (q_c) to the initial mean effective stress applied to the soil on the commencement of the tests (p'_i). The rate of pore pressure generation during cyclic loading is the second common outcome of these laboratory tests. These two main characteristics will be used to incorporate the effects of cyclic loading into the liquefaction analyses presented herein.

3. CONSTITUTIVE MODEL

The proposed constitutive model is based on the well-known elastic–perfectly plastic Mohr–Coulomb soil model. The effects of cyclic loading are included by a suitable modification of the stress–strain relationship.

In the Mohr–Coulomb model the yield surface and failure surface coincide, and both are constant in the stress space. Under monotonic loading the yield surface defines the stress conditions under which plastic deformation occurs for the soil. It also separates zones of elastic behaviour from those of plastic behaviour. Stress paths within the yield surface result in purely recoverable (elastic) deformations, while paths which intersect the yield surface produce both recoverable and permanent (plastic) deformations. This model, in its standard form, is not suitable for cyclic loading, since within a constant yield surface no amount of stress cycling can produce any permanent strains. However, the Mohr–Coulomb model can be extended to incorporate the effects of cyclic loading. This extension is achieved by including some plastic deformations when the state of stress is inside the yield locus. When the state of stress reaches the failure surfaces, under either monotonic or cyclic loading, the soil behaviour is defined by the Mohr–Coulomb model and the cyclic load is considered to have no further effect on the soil response, i.e. the element of soil is at plastic failure.

Within the framework of the theory of plasticity, the total strain increment, $d\varepsilon$, is decomposed into the elastic strain increment, $d\varepsilon^e$, and the plastic strain increment, $d\varepsilon^p$, by a simple superposition, i.e.

$$d\varepsilon = d\varepsilon^e + d\varepsilon^p \tag{1}$$

Under monotonic loading, the elastic strain increment is assumed to be completely described by Hooke's law where, for an isotropic material, two material parameters, such as Young's modulus and Poisson's ratio, are constant. Plastic yielding in the soil is determined by the Mohr–Coulomb criterion. Once plastic yielding commences, the relative magnitudes of the plastic strains are obtained from the flow rule.

Under cyclic loading, another component of plastic strain increment, which is the direct result of cyclic loading only, $d\varepsilon^c$, is added to Equation (1), i.e. the total strain may be written as

$$d\varepsilon = d\varepsilon^e + d\varepsilon^p + d\varepsilon^c \tag{2}$$

The general incremental stress–strain relationship can be given as

$$d\sigma' = \mathbf{D}(d\varepsilon - d\varepsilon^c) \tag{3}$$

or alternatively as

$$d\sigma - e\, du = \mathbf{D}\, d\varepsilon - \mathbf{D}\, d\varepsilon^c \tag{4}$$

where $\mathbf{D}$ is the stiffness matrix of the soil skeleton, u is pore pressure, σ and σ' are vectors of total stress and effective stress, respectively, and $e = (1, 1, 1, 0, 0, 0)^T$.

Computationally, the term $d\varepsilon^c$ (or $\mathbf{D}\, d\varepsilon^c$) in Equation (4) can be regarded as an initial strain (or initial stress) in the standard finite element formulation of consolidation. The effects of this extra term in the right-hand side vector of the finite element equation are similar to the effects of application of additional forces to the soil mass. These extra forces would produce excess pore pressures under undrained conditions, or permanent volume strains with consequent settlements under drained conditions or a combination of excess pore pressures and settlements under partially drained conditions, such as the conditions frequently encountered in soils under offshore foundations.

The additional plastic strains produced during drained cyclic loading can be obtained from experimental tests on samples of soil. The plastic strains resulting from cyclic drained tests can be used directly in the finite element formulation. However, cyclic tests are usually carried out on saturated samples of soil under undrained conditions and the generated excess pore pressures are recorded during these experiments. The pore pressures can be related to the plastic strains by the following equation [1]:

$$d\varepsilon^c = ee^T\mathbf{D}^{-1}e\, du_c/3 \tag{5}$$

where u_c is the pore pressure generated due to cyclic loading under undrained conditions and ε^c is the corresponding plastic strain which is produced by cyclic loading under fully drained conditions. An important consequence of Equation (5) is that the cyclic strain and the pore water pressure induced by cyclic loading can be used interchangeably in all computation, provided that the inverse of the stiffness matrix exists. In the Mohr–Coulomb model $\mathbf{D}^{-1}$ can be evaluated before the ultimate failure state. When the stress state reaches the failure conditions, $\mathbf{D}^{-1}$ may no longer exist. In this case it is assumed that cyclic loading has no further effect on the behaviour of the soil.

For any isotropic elastic stiffness matrix, it can be shown that

$$\mathbf{D}ee^T\mathbf{D}^{-1} = 3. \tag{6}$$

Substituting Equation (6) into Equation (5) results in

$$\mathbf{D}\mathrm{d}\varepsilon^{\mathrm{c}} = e\,\mathrm{d}u_{\mathrm{c}} \tag{7}$$

Equation (4) can therefore be written in a form suitable for the direct use of the pore pressures generated due to undrained cyclic loading as follows:

$$\mathrm{d}\sigma - e\,\mathrm{d}u = \mathbf{D}\,\mathrm{d}\varepsilon - e\,\mathrm{d}u_{\mathrm{c}} \tag{8}$$

Where the results of undrained cyclic tests are expressed in term of excess pore pressure, the rate of generation of pore pressure should also include the effects of any possible non-linearity in soil behaviour. In other words, the results of undrained cyclic tests with pore pressure measurement capture the non-linearity of the behaviour of the soil skeleton before the onset of liquefaction or failure. Therefore, the elastic-perfectly plastic model together with the experimental data obtained on samples of saturated soil should provide a reasonable representation of the soil behaviour under cyclic loading.

4. METHOD OF LIQUEFACTION ANALYSIS OF OFFSHORE FOUNDATIONS

The method presented here for liquefaction analysis of offshore foundations consists of a sequence of the generation of pore pressure under undrained conditions followed by the dissipation of pore pressure under partially drained conditions. This includes several steps, viz., the definition of a design storm, the computation of initial stresses in the soil under ambient loads, the computation of cyclic stresses in the soil continuum, the prediction of excess pore pressures generated by cyclic loading, and the computation of the dissipation of the pore pressure.

Typically, the design storm is divided into a number of parcels of waves of equal height. For each wave parcel the distribution of cyclic stresses developed below the sea floor is estimated. Based on the cyclic stress ratio, the increment in excess pore pressure generated due to an increment in load cycles during a time interval Δt is evaluated, assuming undrained conditions. This step requires the results of laboratory tests and will be discussed in detail in a subsequent section. The increment in excess pore pressure is then included in the finite element equations of consolidation. These are subsequently solved for the dissipation of the pore pressure and the associated changes in stresses and displacements. The process of the generation and dissipation of pore pressure is followed for all parcels of waves until the end of the storm. A schematic representation of the liquefaction analysis is presented in Figure 2.

5. CALCULATION OF PORE PRESSURE

In the finite element analysis of liquefaction, the excess pore pressure generated by the application of any specific number of cycles of load must be calculated and substituted in Equation (8). This is possible using the results of laboratory tests on saturated samples of soil performed under undrained conditions. Since the stress paths which are followed by elements of soil in a boundary value problem are not as simple as those applied in laboratory tests, a special scheme to allow estimation of the appropriate pore pressure increment is required.

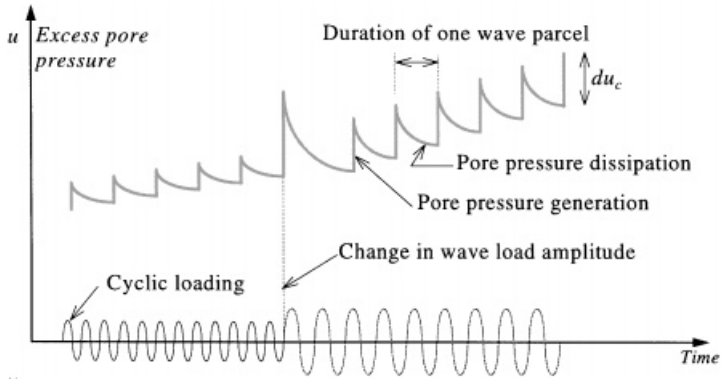

Figure 2. Schematic representation of the generation and dissipation of pore pressure in a liquefaction analysis.

To evaluate the excess pore pressure generated in the soil due to cyclic loading, it is convenient to view cyclic loading as an agent that causes 'damage' to the shearing resistance of the soil skeleton. As the pore pressure increases, the shearing capacity of the soil reduces. Eventually, the shearing resistance of the soil may reduce to a value equal to the shear stress applied to the soil by ambient loads. At this stage, the state of stress would be on the failure locus where further reduction in the effective stress or further increase in the loads would cause unlimited plastic shearing. This stage can be regarded as the onset of liquefaction.

At any stage during cyclic loading the amount of damage done to the soil structure can be evaluated by a damage index, DI, which is conveniently defined as follows:

$$\mathrm{DI} = (S_\mathrm{i} - S_\mathrm{c})/S_\mathrm{i} \tag{9}$$

where S_i is the 'extra' shearing capacity of the soil at the initial conditions, i.e. at the beginning of a liquefaction analysis where the soil is under ambient loads only, S_c is the extra shearing capacity of the soil at any stage during the analysis. Both S_i and S_c can be evaluated by the initial and current values of the mean effective stress and the position of the failure surface, as shown in Figure 3.

The damage index, DI, ranges from zero to one. While $\mathrm{DI} = 0$ indicates that no damage has been done to the soil by cyclic loading, $\mathrm{DI} = 1$ represents full damage to the soil structure and therefore liquefaction failure. When $\mathrm{DI} = 1$, the soil does not have any further resistance to shear loading, and if unrestrained under the current load, it would show an infinite shearing displacement. It is worth noting that the damage index is equal to the ratio of the generated excess pore pressure, u_c, to the maximum achievable pore pressure before failure, u_max. In undrained cyclic tests, u_max is the horizontal distance between the initial state and failure state in the p'–q space (Figure 3). It is precisely because of this equivalence between the pore pressure ratio ($u_\mathrm{c}/u_\mathrm{max}$) and the damage index (DI), defined in terms of the available shearing resistance (S_i and S_c), that the proposed definition of DI has been preferred over possible alternatives based on, for example, the stress ratio (q/p').

The increment of excess pore pressure generated by any specific number of cycles of load can be estimated provided that the rate of damage is determined. The rate of damage done to the soil structure can be taken equal to the rate of the generation of pore pressure under undrained

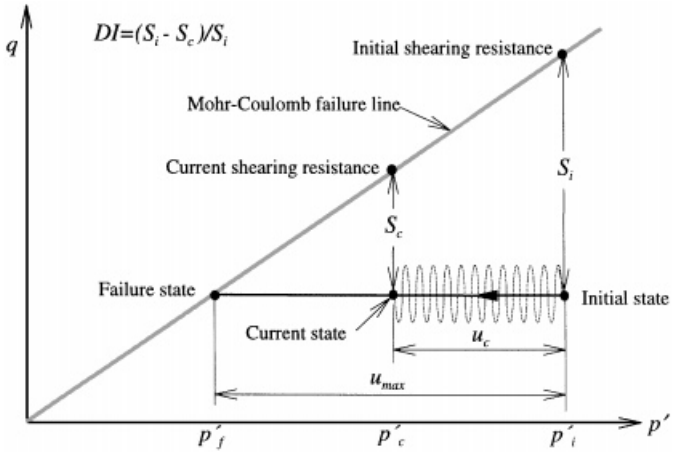

Figure 3. Definition of 'damage index' for a soil element under cyclic loading and undrained conditions.

conditions, obtained from laboratory cyclic tests. As an example, the rate of pore pressure generation was suggested by Seed *et al.* [2] as

$$\frac{u_c}{u_{max}} = \frac{2}{\pi} \arcsin\left(\left(\frac{N}{N_1}\right)^{1/2\alpha}\right) \tag{10}$$

where u_c is the excess pore pressure generated due to application of N load cycles, u_{max} is the pore pressure which will be generated at failure when N_1 load cycles is applied to the soil, and α is a pore pressure generation parameter. For any soil N_1 can be determined from cyclic laboratory tests under undrained conditions.

The increment in pore pressure generated due to an increment in load cycles, ΔN, under undrained conditions can now be evaluated from Equation (10) as

$$\frac{du_c}{u_{max}} = \frac{2}{\pi} \arcsin\left(\left(\frac{N + \Delta N}{N_1}\right)^{1/2\alpha}\right) - \frac{u}{u_{max}} \tag{11}$$

where u is the current value of excess pore pressure generated due to the cyclic loads applied to the soil up to the current time. As indicated previously, the pore pressure ratio is equal to the damage index, i.e., $u_c/u_{max} = \mathrm{DI}$. Therefore, the increment in excess pore pressure generated by an increment in load cycles under undrained conditions can be evaluated by the following expression:

$$\frac{du_c}{u_{max}} = \frac{2}{\pi} \arcsin\left(\left(\frac{N + \Delta N}{N_1}\right)^{1/2\alpha}\right) - \mathrm{DI} \tag{12}$$

Unlike standard cyclic tests, the cyclic stresses in a boundary value problem usually vary with both position and time, based on the intensity and nature of the applied cyclic loads. The drainage conditions in a boundary value problem also allow some of the excess pore pressures generated due to the cyclic loading to be dissipated and, as a consequence, some of the shearing resistance of the soil to be recovered. The effects of drainage and previous cyclic load experience can be directly related to the amount of damage done to the soil shearing resistance. To do so, an

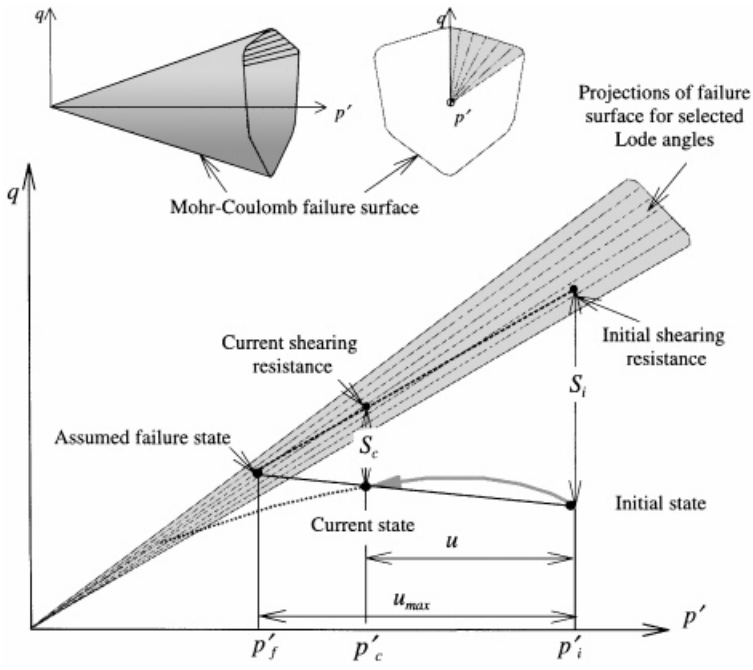

Figure 4. Stress path in the field and prediction of failure point.

equivalent cyclic ratio, R_N, is defined as follows:

$$R_N = \left(\sin\left(\frac{\pi \mathrm{DI}}{2}\right)\right)^{2\alpha} \tag{13}$$

Therefore, for the general cases of boundary value problems under partial drainage and where cyclic stresses are not constant, Equation (12) may be replaced by

$$\frac{\mathrm{d}u_c}{u_{\max}} = \frac{2}{\pi}\arcsin\left(\left(R_N + \frac{\Delta N}{N_1}\right)^{1/2\alpha}\right) - \mathrm{DI} \tag{14}$$

In Equations (12)–(14), DI is the cumulative damage done previously to the soil.

Application of Equation (14) for calculation of excess pore pressures in a boundary value problem requires some idealisations. Unlike in laboratory tests, the stress paths and therefore the maximum achievable pore pressures are not pre-determined in boundary value problems. However, a simple extrapolation, between the initial state of stress and the current state of stress to the failure surface, allows the prediction of the failure state and therefore the approximation of the maximum achievable pore pressure. This procedure is shown schematically in Figure 4. In this figure a probable stress path in the field is illustrated in the Cambridge p'–q space, together with the projections of the Mohr–Coulomb failure surface for selected Lode angles.

The maximum achievable pore pressure can be calculated from the properties of the similar triangles in Figure 4, i.e.

$$u_{\max} = \frac{uS_i}{S_i - S_c} = \frac{u}{\mathrm{DI}} \tag{15}$$

In some special cases the value of $u_{\max}$ cannot be calculated form Equation (15). For example, at the beginning of a liquefaction analysis or where the stress path moves parallel to the failure surface, where $S_i = S_c$. In these cases the maximum achievable pore pressure is taken as the horizontal distance between the initial state of stress and the failure surface. In some other cases the mean effective stress increases during cyclic loading and therefore, the damage index may be calculated to be less than zero. In these situations, DI is taken as zero, assuming no significant damage has been done to the soil shearing resistance, and $u_{\max}$ is taken as the horizontal distance between the initial state of stress and the failure surface.

6. ILLUSTRATIVE EXAMPLE

The method described in this paper was used to analyse the foundation of the Ekofisk tank [3] which was constructed in the North Sea in 1973. The tank has been the subject of previous liquefaction analyses, e.g. References [4–8]. The tank was instrumented to measure oceanographic data, pore pressures in the soil, and the settlement and tilt of the tank [3]. Predictions of the liquefaction analysis can therefore be compared with the response observed during a major storm.

6.1. Definition of the problem

The Ekofisk tank is a concrete structure with a diameter of 93 m and a height of 90 m, installed in 70 m of water in the North Sea on June 1973 (Figure 5). The tank was constructed for oil storage to maintain production in bad weather. It has also been used as a production platform. The tank has a horizontal cross section shaped like a square with rounded corners.

The seabed beneath the tank consists of a fine sand to a depth of 26 m. Interbedded in this sand layer at a depth of about 16–18 m is a layer of stiff clay with low plasticity. Below 26 m, hard clays are interbedded with sand layers to a great depth. *In situ* cone penetration tests before installation of the tank indicated that the sand was very dense with a relative density of about 100 per cent in the upper few meters [9]. The permeability of the sand in the Ekofisk field is of the order of 10^{-5} m/s [4]. The coefficient of volume compressibility was estimated as $m_v = 1.73 \times 10^{-5}$ m^2/kN [6]. Assuming a Poisson's ratio of $v = 0.25$, the drained Young's modulus of the sand can be calculated from the value of m_v, as $E' = 48\,000$ kN/m^2. The saturated unit weight of the sand varies between 13.4 and 17.6 kN/m^3. However, a value of $\gamma_{sat} = 17.3$ kN/m^3, which was used by Rahman *et al.* [6] is also adopted in this study. The initial value of the coefficient of lateral earth pressure is assumed to be $K_0 = 0.5$.

A typical value of the friction angle for the sand in the Ekofisk field, obtained in drained triaxial tests, is $\phi = 43^\circ$ [4]. The dilation angle for the sand is assumed to be zero. Therefore, a non-associated flow rule is assumed for the sand based on the elasto-plastic model. This implies that under drained conditions there will be no plastic volume change under monotonic shearing.

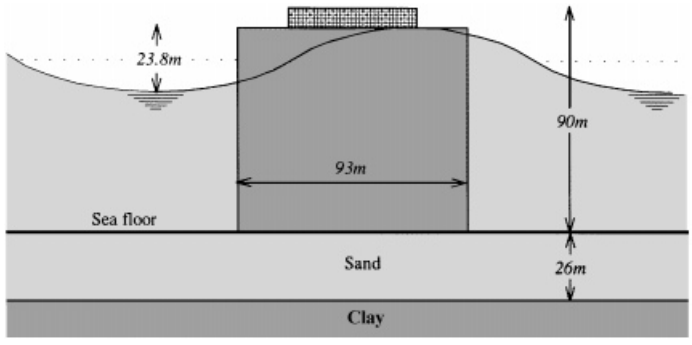

Figure 5. Geometry of the Ekofisk tank.

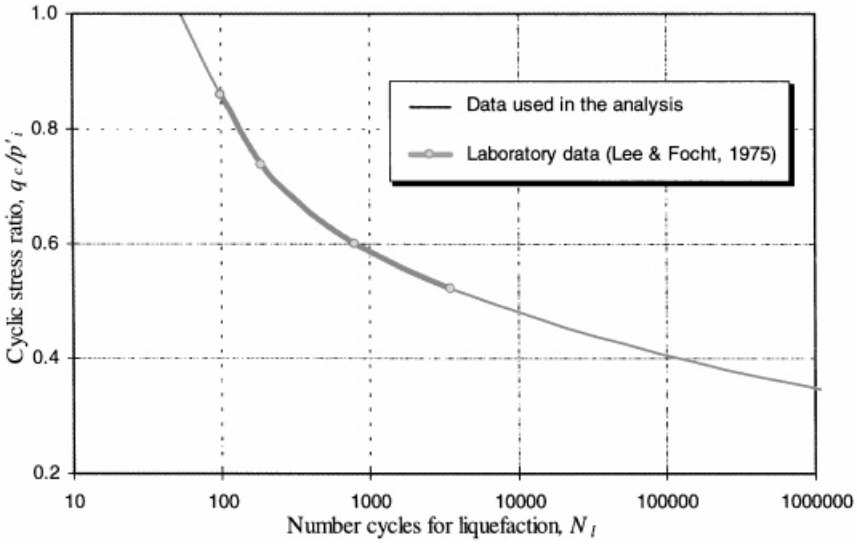

Figure 6. Liquefaction characteristics of the Ekofisk sand.

A series of undrained cyclic triaxial tests on saturated samples of sands from the Ekofisk field has been performed by Lee and Focht [5]. The results of the tests are presented in Figure 6, together with the idealization used in the present analysis. It was assumed that the rate of pore pressure generation, or the rate of damage, during cyclic loading can be adequately represented by Equation (10) with a pore pressure parameter of $\alpha = 0.7$.

The design storm has a return period of 100 y. The histogram of the storm, as presented by Rahman *et al.* [6] is shown in Figure 7.

The submerged weight of the Ekofisk tank is about 1900 MN. The forces that are generated by the storm waves have been evaluated by Rahman *et al.* [6] and are shown in Figure 8. The effects of cyclic vertical force were found to be very small and this force is therefore ignored in the analysis.

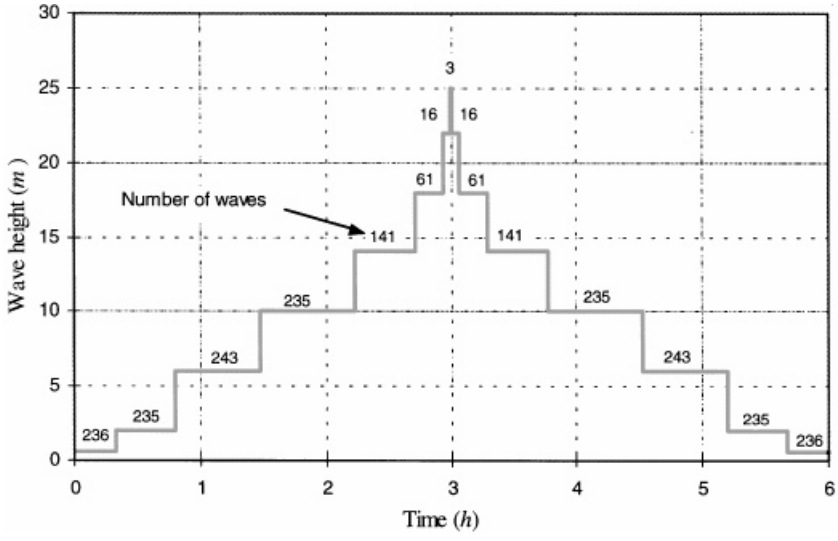

Figure 7. Histogram of the 100 yr design storm.

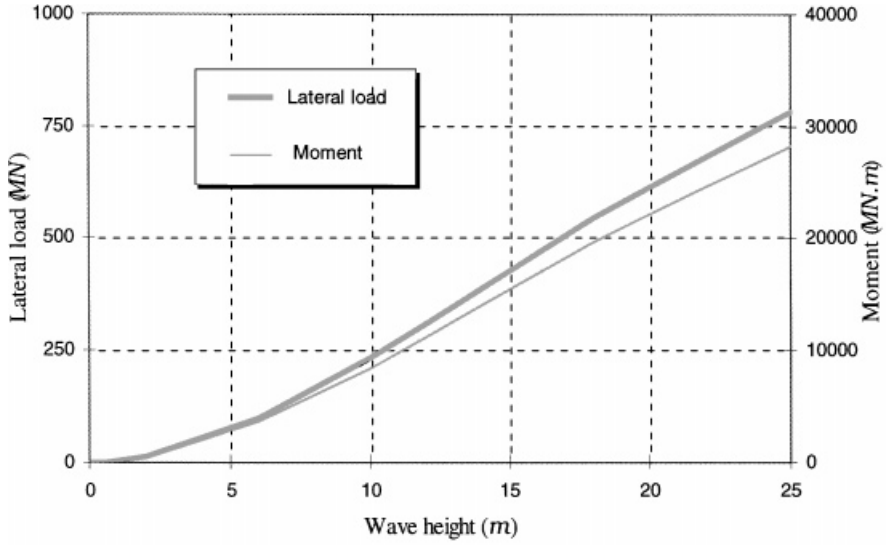

Figure 8. Variation of cyclic lateral load and moment with wave height.

6.2. *Finite element idealization*

In a liquefaction analysis the whole process of generation and dissipation of pore pressure must be followed hundreds of times. Application of a standard three-dimensional finite element method in a liquefaction analysis requires enormous computational time. In order to increase the efficiency of the liquefaction analysis, a semi-analytical approach [10] has been used to develop

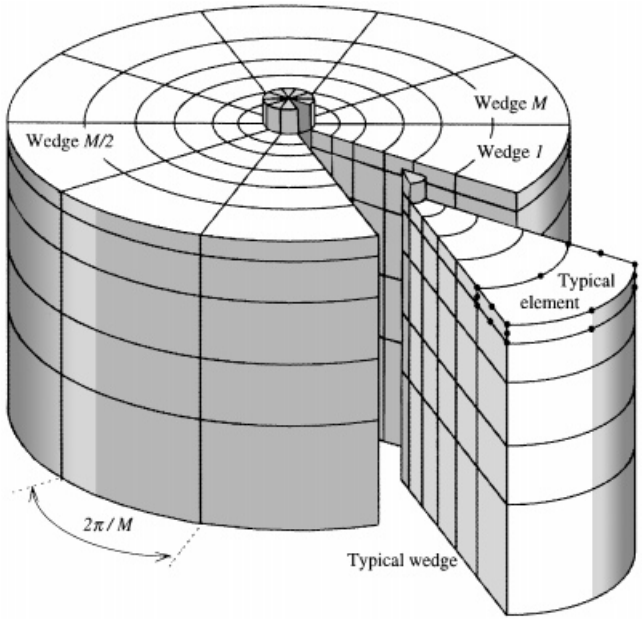

Figure 9. Finite element idealization.

a finite element program capable of performing a three-dimensional consolidation analysis. This approach is based on the assumption that the field quantities such as displacements and pore pressure can be represented by their discrete Fourier transforms. In this method advantage is taken of the axi-symmetric nature of the problem geometry, and only one wedge from a cylinder of the soil-foundation materials requires modelling (Figure 9). Instead of solving a very large number of algebraic equations for the full three-dimensional problem, a smaller number of equations arising from a substitute problem are solved [1]. This method reduces the computational time to less than 5 per cent of the time required for a standard three-dimensional finite element solution.

The finite element mesh used in the analysis of the Ekofisk tank is presented in diametral cross-section in Figure 10. In order to reduce the effects of rigid boundaries on the stress distribution within the sand layer, a 24 m thick layer of clay, with the same elastic properties as the sand, was included in the mesh under the sand layer. The clay layer and the interface between the foundation and the sand were assumed to be impermeable. Perfect drainage was assumed on the remaining parts of the boundary.

6.3. Soil failure during the storm

The predicted changes in the state of the soil under the tank during the storm are shown in Figure 11, where the zones of failed soil are presented sequentially. Under the ambient load, at time = 0.0, the soil under the edge of the tank fails (becomes plastic) under compressive stresses while the soil close to the surface adjacent to the tank is predicted to fail in tension. After the

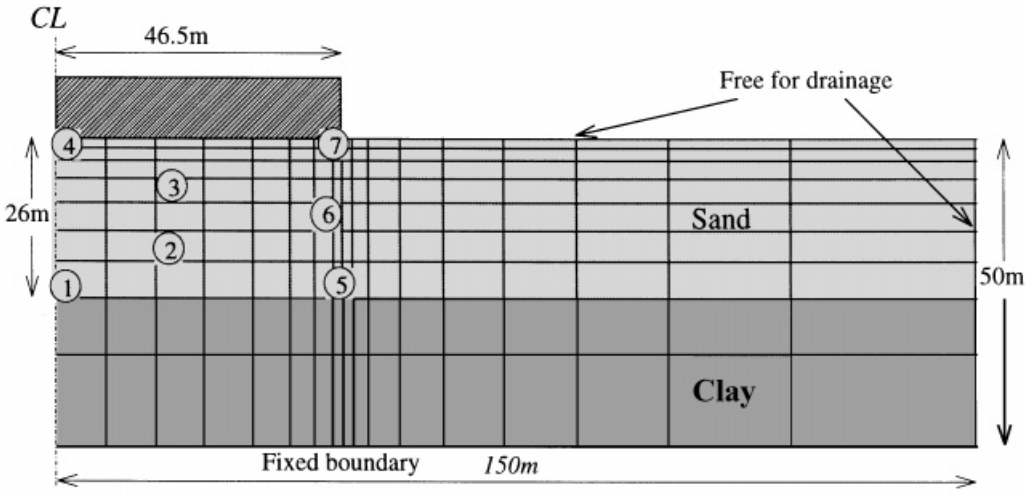

Figure 10. Finite element mesh for Ekofisk tank.

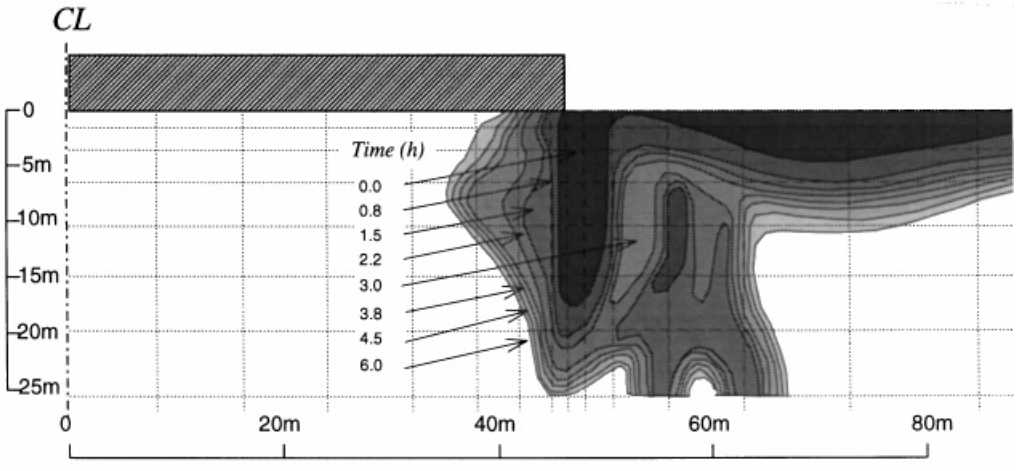

Figure 11. Expansion of failure zone during the storm.

application of cyclic load, the pore pressures inside the soil rise and cause redistribution of stresses in the soil elements and reduction of soil shearing strength. The redistribution of stresses may decreases the effective stresses in some elements and cause the elements to yield plastically. The reduction in the shearing resistance of some points in the soil may also result in the plastic failure of those points. Since both redistribution of stresses and reduction in soil shearing resistance originate from the application of cyclic loading, the failure zones which are produced during storm loading can be regarded as "liquefaction-induced failure". From Figure 11, it may

be observed that the soil elements under the edge of the foundation and also the elements close to the surface adjacent to the tank are the most critical elements during storm loading.

6.4. *Variation of pore pressures*

Variations of the excess pore pressures during storm loading for some representative points in the soil under the foundation are presented in Figure 12. The position of these points in the sand layer are shown in Figure 10. The pore pressure reaches 47 kPa at the centre of the foundation, 3.8 h after the beginning of the storm. The pore pressure under the edge of the footing, 1.5 m below the soil surface, reaches a maximum value of about 10 kPa.

There is a fluctuation in the predicted pore pressure under the edge of the tank. This behaviour was observed for the points which reach the yield surface during cyclic loading and is an artifice of the numerical solution scheme. When the state of stress is on or near the yield surface, the isotropic increase in excess pore pressure due to cyclic loading decreases the mean effective stress and causes the state of stresses to drift from the yield surface. The process of bringing the state of stresses back to the yield surface generally changes the stresses, which in turn affects the excess pore pressure. During cyclic loading, the continuous correction of stresses corresponding to a point on the yield surface results in the numerical fluctuation of the pore pressure at that point.

The distributions of excess pore pressures predicted in the sand layer are presented in Figures 13 to 16 at 1.5, 3.0, 3.8 and 6.0 h after the beginning of the storm. The maximum pore pressure at time 1.5 h is about 38 kPa which is generated close to the clay layer, about 55 m away from the

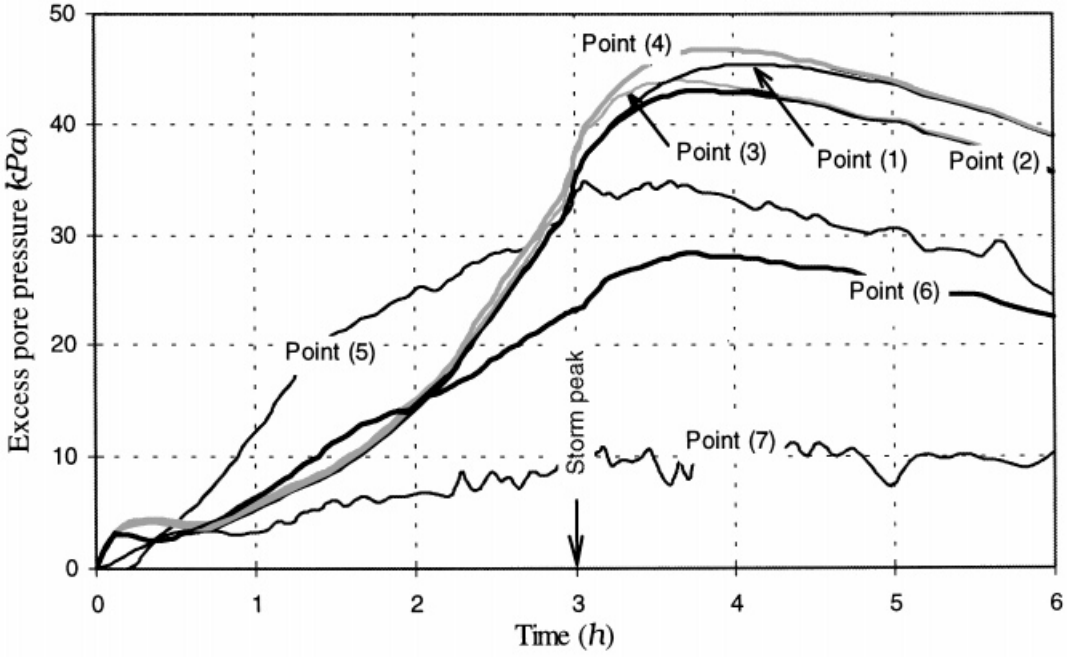

Figure 12. Variation of excess pore pressures for representative points.

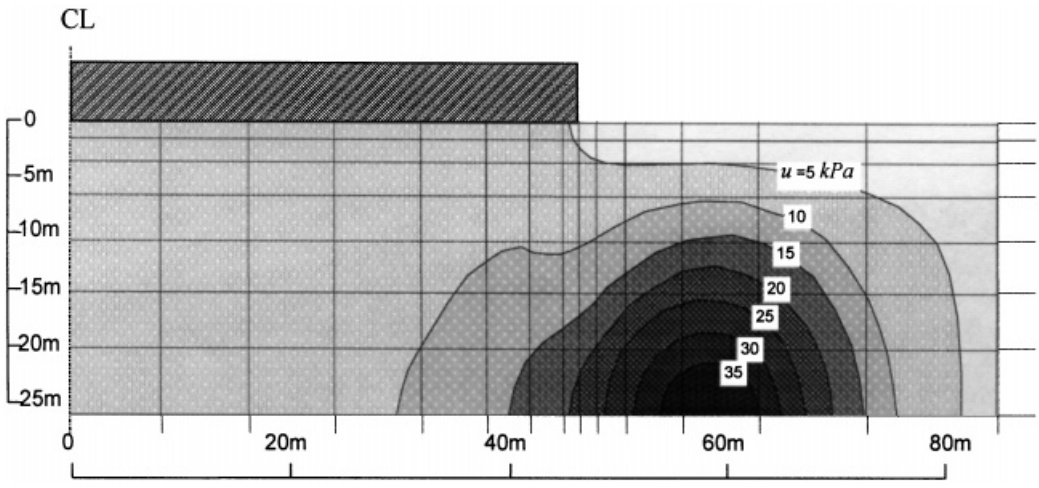

Figure 13. Distribution of excess pore pressure at time = 1.5 h.

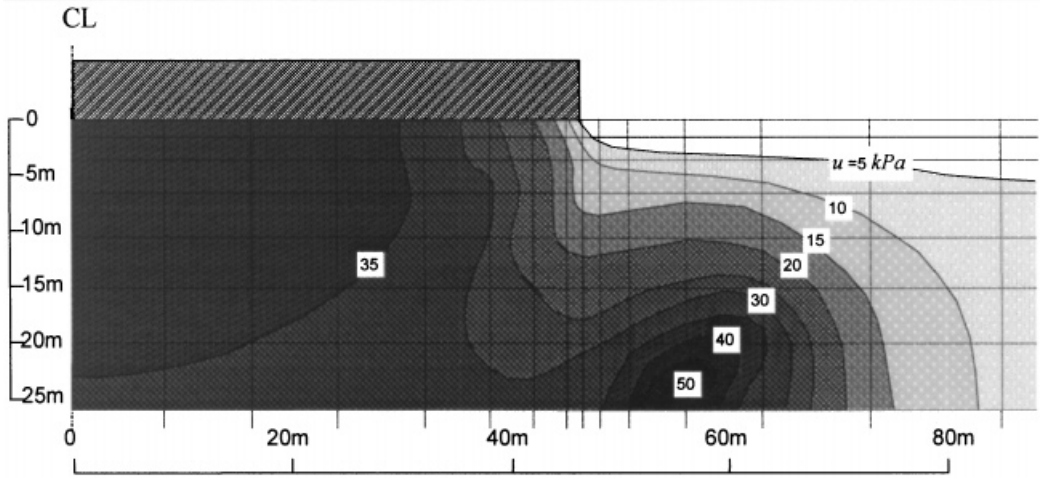

Figure 14. Distribution of excess pore pressure at time = 3.0 h.

centre of the tank (Figure 13). The maximum pore pressure predicted during the storm reaches approximately 51 kPa, Figure 14, which is generated at the storm peak. The pore pressure beneath the tank rises to 47 kPa, at time 3.8 h (Figure 15), and after that the pore pressure reduces. At the end of the storm there exists a substantial residual pore pressure under the tank (Figure 16), with a maximum of 39 kPa which is generated at the centre of the tank.

The value of the excess pore pressure under the edge of the tank is not very high. However, the soil elements under the edge are mostly at critical state, since they experience relatively large

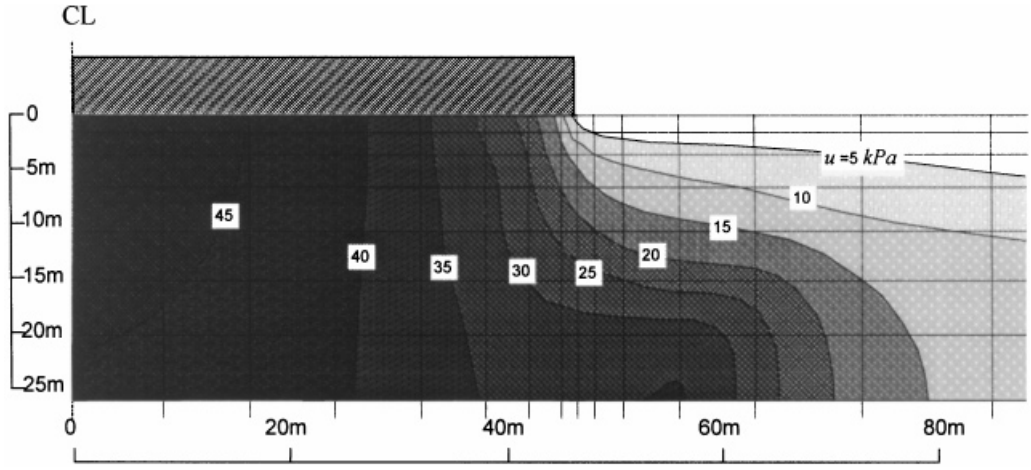

Figure 15. Distribution of excess pore pressure at time = 3.8 h.

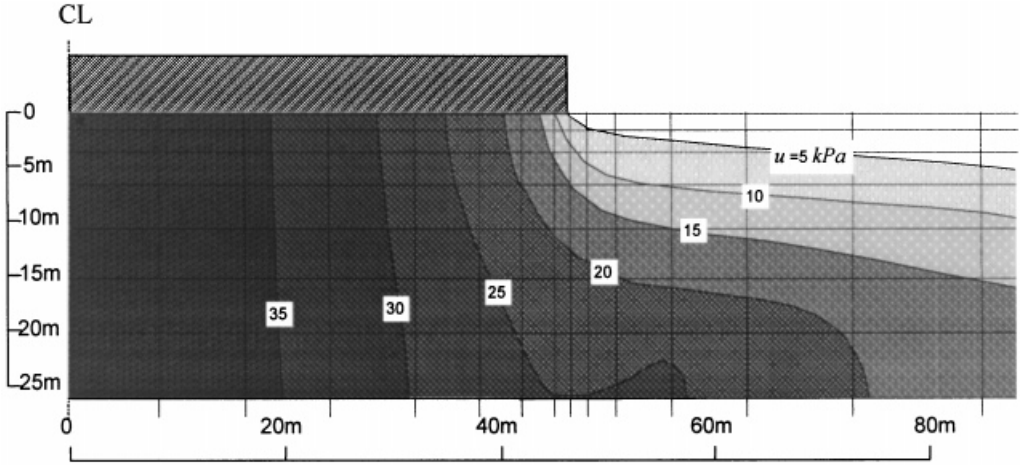

Figure 16. Distribution of excess pore pressure at time = 6.0 h.

deviator stresses and fail under the ambient loads. The model for liquefaction does not generate any further pore pressure for elements of soil which are at the failure state. However, the diffusion of water from zones of high pressure under the tank toward the free drainage boundaries causes the pore pressure in the elements under the edge of the tank to be increased before final dissipation.

6.5. Stress paths

The effective stress paths of the representative points during storm loading are presented in Figures 17 and 18. A portion of the Mohr–Coulomb failure surface, which is between the extreme

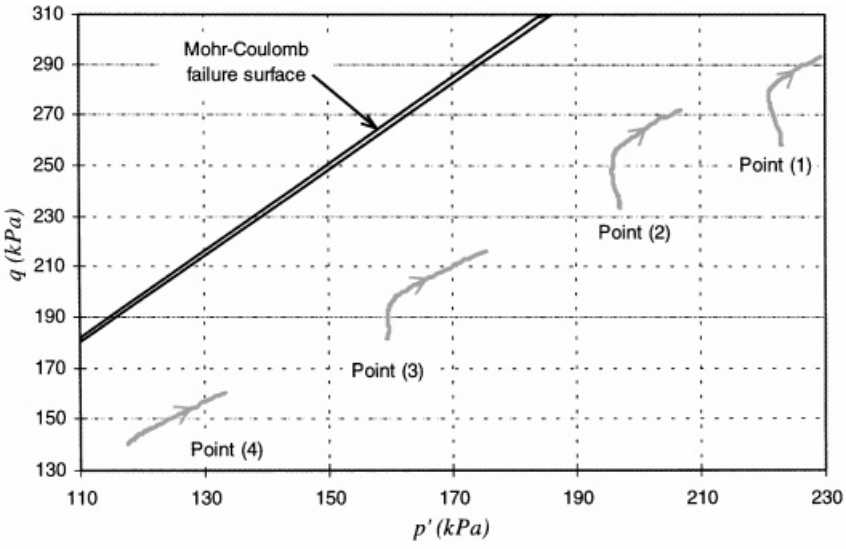

Figure 17. Stress paths for points (1)–(4).

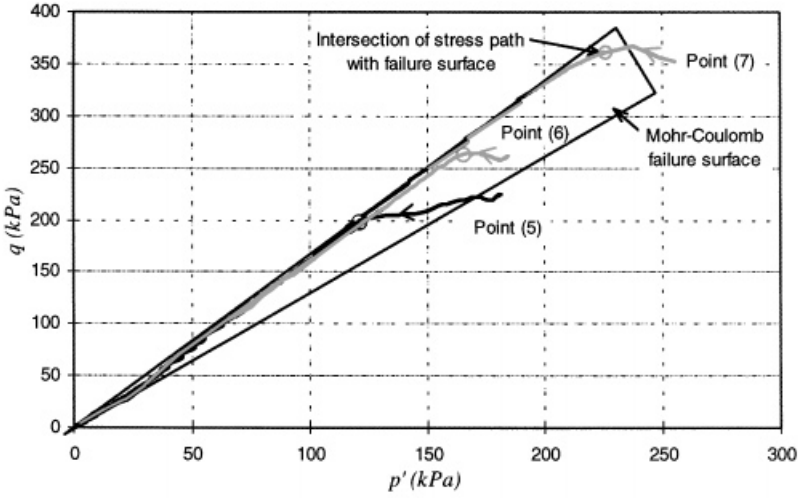

Figure 18. Stress paths for points (5)–(7).

ranges of the Lode angles corresponding to the stresses, is also shown in these figures. Points (1)–(4) are under the middle part of the foundation. The states of stresses at these points are all inside the yield locus at the beginning of the storm and stay elastic during cyclic loading. The stress paths show upward movements with an increase in the deviator stresses. The mean effective stresses at these points decrease slightly and then increase later during the storm (Figure 17).

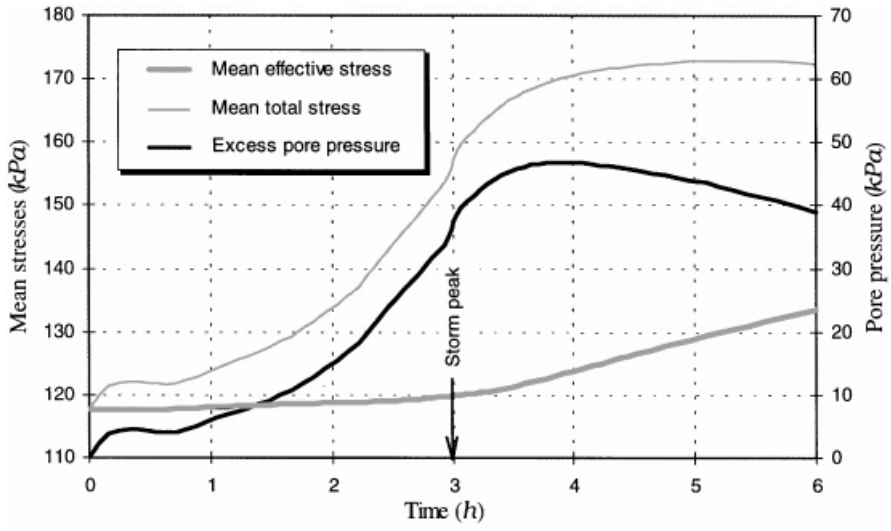

Figure 19. Variations of the mean effective stress, the total stress and the excess pore pressure for a point at the centre of the tank.

Points (5)–(7) are under the edge of the foundation. The states of stresses of these points are inside the yield locus at the beginning of the storm. However, the stress paths move toward the failure surface during the storm, decreasing the mean effective stresses, and therefore the shearing resistance of the soil, and eventually the points fail (Figure 18). The intersections of the stress paths with the failure surface are marked by circles in Figure 18. After failure, the stress paths move down, along the failure surface, decreasing both the mean effective stresses and the deviatoric shear stresses.

Stress redistribution in the soil under a foundation is an important aspect of cyclic loading. If the total stress in the soil does not change, the mean effective stress should be reduced continuously during pore pressure build-up. However, the results of the present analysis show that the mean effective stresses increase in some elements of the soil. To illustrate the stress redistribution in the soil during cyclic loading, the predicted variations of the mean effective stress, the pore pressure, and the mean total stress for a point close to the centre of the foundation, point (4), are plotted in Figure 19. The total mean stress increases sharply before the storm peak, almost at the same rate as the increase in excess pore water pressure, while the change in the mean effective stress is negligible. This indicates that the increase in excess pore pressure at this point is mainly due to the redistribution of stresses inside the soil. After the storm peak, the rate of increase in the mean total stress reduces and the dissipation of pore water pressure increases the mean effective stress.

6.6. Settlement

The predicted variation of the settlement of the tank during the storm loading is presented in Figure 20. During the storm, especially during the application of wave loads with high intensities,

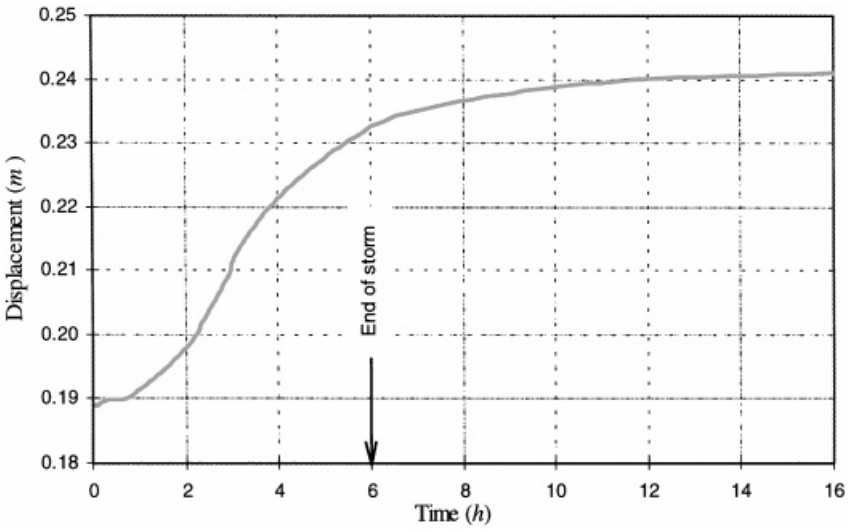

Figure 20. Displacement of the tank during cyclic loading.

the displacement increases. The foundation continues to settle up to 10 h after the end of the storm. Overall, the settlement of the foundation is predicted to increase by approximately 0.052 m as a result of the storm.

6.7. Evaluation of the numerical predictions

The results of the analysis of the tank can be compared with the observed responses of the tank during two major storms. One of the major storms occurred on 6 November 1973, during which the performance of the foundation was measured. The storm had a maximum wave height of about 16 m and caused the pore pressure in the upper layer of the sand to be increased by 10–20 kPa [3]. The most severe storm occurred on 19 November 1973 during which the recording system was out of operation. The severity of the storm was estimated based on visual observations from a weather ship 100 km away from the tank. The maximum wave height generated by this storm was probably 21 m. During the first storm on 6 November, the tank probably settled 0.02 m [3]. During the period of severe storms, 15–20 November, the tank settled an additional 0.03–0.05 m. Assuming that the excess pore water pressures are proportional to the settlements, Clausen *et al.* estimated that a maximum pore pressure of about 40 kPa was generated under the tank on 19 November.

The liquefaction analysis reported here was performed for a 100 y design storm. This design storm has three maximum waves with a height of 24 m and, therefore, is probably more severe than the storm that occurred on 19 November. The predicted pore pressures under the tank reached 51 kPa during the storm. The additional settlement of the tank due to the storm loading was also predicted as 0.052 m. Taking into account the severity of the design storm, in comparison with the storms on 6 and 19 November, the predicted pore pressures and the settlement of the tank are considered reasonable.

7. CONCLUSIONS

A simple extension to an elasto-plastic model for soil, suitable to be used in a liquefaction analysis, has been presented. The model is based on the Mohr–Coulomb failure criteria. To incorporate the effects of cyclic loading, additional plastic volumetric strains are included in the model by utilising experimental data obtained from laboratory cyclic loading tests on soil.

The elasto-plastic model was employed in a liquefaction analysis of the Ekofisk tank. The pore pressure predicted at the centre of the tank is about 20 per cent greater than the estimated pore pressure generated by a severe storm. This storm had a probable maximum wave height of about 21 m, corresponding to 90 per cent of the 100 y design storm wave. The predicted settlement of the foundation is also slightly larger than the maximum 'observed' settlement during the severe storm. Therefore, the performance of the finite element model can be regarded as satisfactory.

Application of the elasto-plastic soil model represents an improvement on more traditional methods of liquefaction analyses of offshore foundations. In previous analyses, employing an elastic soil model, some elements of the soil exhibit unrealistic stress paths with negative mean effective stresses [1], a situation that is unlikely to be sustained in the ground. Another improvement in using an elasto-plastic model is that the redistribution of stresses in the soil during cyclic loading can be reasonably predicted. This will lead to a better prediction of the settlement of the foundations. Obviously, even more accurate elasto-plastic models may result in better predictions of the soil behaviour. It is noted that the generalized equation describing the stress–strain relationship in a liquefaction analysis can be used with any kind of soil model. The yield criteria and the flow rules offered by any model can be associated with appropriate experimental data for cyclic loading and used in the liquefaction analyses. However, it is believed that the experimental data usually capture the important non-linearity associated with the cyclic behaviour of soil. Therefore, a simple elasto-plastic formulation, such as the one presented in this paper, is probably adequate in representing soil behaviour under cyclic loading, for the solution of many practical problems. This conclusion is certainly applicable to the case study considered in this paper, but further case studies are required to confirm if it is more widely applicable.

ACKNOWLEDGEMENTS

The research described in this paper was conducted as a part of the work of the Special Research Centre for Offshore Foundation Systems, established and supported under the Australian Research Council's Research Centres Program. Financial support from the Centre for Geotechnical Research at the University of Sydney is also gratefully acknowledged.

REFERENCES

1. Taiebat HA. Three dimensional liquefaction analysis of offshore foundation. *Ph.D. Thesis*, The University of Sydney, Australia, 1999.
2. Seed HB, Martin PP, Lysmer J. The generation and dissipation of pore water pressure during soil liquefaction. *Report No. EERC75-26*, Earthquake Engineering Research Center, The University of California, Berkeley, 1975.
3. Clausen CJF, Dibiagio E, Duncan JM, Andersen KH. Observed behaviour of the Ekofisk oil storage tank foundation. *Proceedings of the Seventh Offshore Technology Conference*, Houston, Vol. 3, 1975; 399–413.
4. Bjerrum L. Geotechnical problems involved in foundations of structures in the North Sea. *Geotechnique* 1973; **23**(3): 319–358.

5. Lee KL, Focht JA. Liquefaction potential at Ekofisk tank in North Sea. *Journal of the Geotechnical Engineering Division, ASCE* 1975; **101**(GT1):1–18.
6. Rahman MS, Seed HB, Booker JR. Pore pressure development under offshore gravity structures. *Journal of the Geotechnical Engineering Division, ASCE* 1977; **103**(GT12):1419–1436.
7. Verruijt A, Song EX. Finite element analysis of pore pressure build-up due to cyclic loading. In *Deformation of Soils and Displacement of Structures. Proceedings of the 10th European Conference on Soil Mechanics and Foundation Engineering*, 1991; 277–280.
8. Bouckovalas G. Ekofisk tank: performance prediction during the storm of Nov. 6, 1973. In *Deformation of Soils and Displacement of Structures, Proceedings of 10th European Conference on Soil Mechanics and Foundation Engineering*, 1991; 1311–1314.
9. Andersen KH. Foundation design of offshore gravity structures. In *Cyclic Loading of Soil: From Theory to Design*, O'Reilly, Brown (eds). Blackie: London, 1991; 122–173.
10. Zienkiewicz OC, Taylor RL. *The Finite Element Method* (4th edn), McGraw-Hill; New York, 1989.

